PIV-INVESTIGATIONS OF INTERNAL SLIT NOZZLE FLOWS AND THEIR INFLUENCE ON LIQUID SHEET BREAKUP

J. Scholz, K. Roetmann, V. Beushausen
Jochen.Scholz@llg.gwdg.de
Laser-Laboratorium Göttingen e.V., Hans-Adolf-Krebs-Weg 1
37077 Göttingen, Germany

Abstract
In this work the influence of the internal flow field on the liquid film was investigated. A strategy for reliable PIV measurements inside of nozzle channels with a height of only a few hundred micrometers and at flow velocities of several m/s has been developed. These PIV measurements provided 2 dimensional snapshots of the velocity field inside the nozzle as well as velocity- and fluctuation-profiles across the channel. The development of the channel flow could be observed along the channel length at laminar and partly turbulent flow conditions. Disturbances were introduced to the flow field by inserting a wire into the channel flow. PIV measurements showed the resulting change of the nozzle flow (in the wake of the wire and without wire, respectively). The resulting effects on the free liquid film were observed using back-lit photographs and perpendicular light-sections through the film surface. In the case of the undisturbed nozzle, velocity fluctuations occurred mainly in the boundary layer and the fluctuations in main streamwise direction were dominant. The free liquid film of this nozzle was smooth at the exit and only at higher *Re* numbers the growth of surface waves could be observed further downstream. The nozzle with inserted wire showed a high level of velocity fluctuation in the center of the flow. Here, the fluctuations normal to the walls were of the same magnitude as the fluctuations in streamwise direction. The liquid film of this nozzle was roughened directly below the nozzle exit, even at low *Re* numbers. The high level fluctuations normal to the wall are assumed to play the dominant role in this process. These measurements demonstrate the influence of the internal flow field on the liquid sheet. The results of the present work agree well with recent experiments of Heukelbach and Tropea [1] and supplement the existing experimental data which for example can be used as input or validation of numerical simulations.

Introduction

Atomization of liquids is of great scientific and industrial interest. In addition to breakup phenomena of liquid jets, the disintegration processes of liquid sheets have been extensively studied in the past decades. A review has been given by Lefebvre [2] in the context of liquid atomization. The disintegration of liquid sheets was treated theoretically for example by Li [3] who used linear instability analysis. In the most recent studies [1][4] the consideration of the internal flow field of the nozzle was included into the investigations of liquid sheet disintegration. Klein et al. [4] examined the influences of the inner flow field on the liquid film breakup by direct numerical simulation (DNS). Their calculations showed that the internal flow conditions of the nozzle like fluctuation- respectively turbulence-level and the average velocity profile have important effects on the stability of the liquid film. Here, the velocity fluctuations normal to the wall (in spanwise direction) should play a dominant roll in the modulation of the free liquid surface. The experimental work of Heukelbach and Tropea [1] demonstrated the influence of the internal flow field on the liquid film in experiments with different slit nozzles. They used laser Doppler velocimetry (LDV) to characterize the internal nozzle flow by velocity- and fluctuation-profiles. Unfortunately, they were only able to measure the fluctuations in the main streamwise direction. The free liquid film was analyzed by back-lit photography.

Also the present work focuses on the interconnection of internal flow field and liquid sheet stability. The main issue is to supplement the existing experimental data with reliable particle image velocimetry (PIV) experiments inside of the nozzle flow. PIV measurements were carried out to obtain two dimensional snapshots of the internal flow field, time averaged velocity profiles and fluctuation profiles for both, the streamwise and the spanwise velocity component. The liquid sheet was observed by back-lit photographs and light-sections, displaying structures and depths of surface waves.

Experimental setup

The central issues of this work are velocity measurements inside the nozzle channel of transparent slit nozzles using Particle Image Velocimetry (PIV). Figure 1 shows the experimental setup schematically. To maintain constant experimental conditions for a long time respectively a long series of single shot measurements, a fluid cycle was used. A rotary pump provided the liquid supply with a maximal counter-pressure of approximately 5 bar (0.5 MPa). Water seeded with tracer particles was used as test liquid. Due to the loss heat of

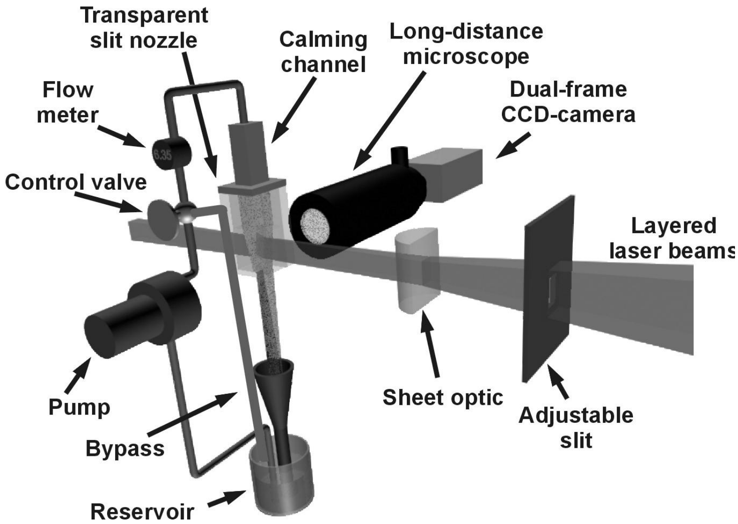

Figure1. Experimental setup for PIV measurements

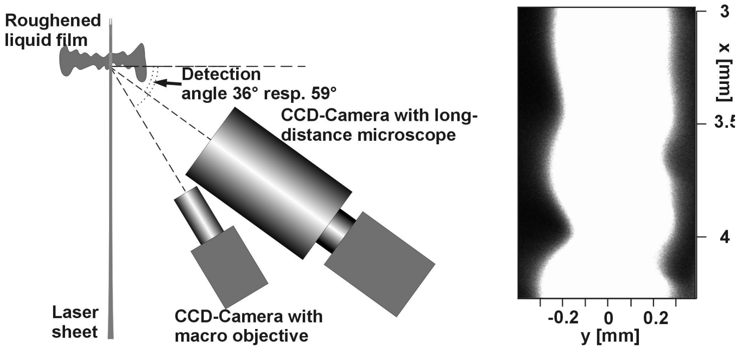

Figure 2. Setup for the light-sheet-fluorescence technique and example of a light-section through the liquid film

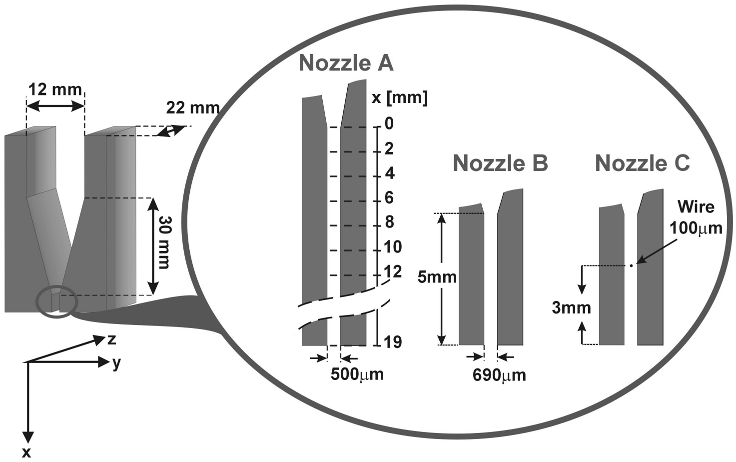

Figure 3. Examined nozzle designs. Up to the nozzle channel all nozzles had the same design.

the pump the water was heated and after a certain operation time a quasi-statical temperature equilibrium was reached. The presented PIV measurements were conducted at an equilibrium water temperature of 35±5 °C, which leads to a kinematic viscosity of $\nu = (0.73 \pm 0.08) \cdot 10^{-6}$ m^2/s [5]. A bypass was used to control the volume flux, which was measured by a flow meter. The replaceable nozzle (description see below) was mounted at the end of a 40 cm long calming channel which had the same inner profile as the nozzle inlet to provide a defined incoming flow. Calming channel and nozzle were held by a micro positioning system. The free liquid stream was caught by a hopper section and led back to the reservoir. This closed circuit allowed constant seeding of the fluid with a defined concentration of tracer particles. Monodisperse glass spheres with a diameter of 1 µm were used as tracer particles (Monospher 1000, Merck KGaA). Advantages of these particles are their defined diameter and that they don't tend to agglomerate in water dispersion.

Figure 1 also sketches the optical setup for PIV measurements. The light of two separately controllable lasers was overlapped collinearly. The laser beams were cut by an adjustable slit aperture and focused with a cylindrical lens (f = 310 mm) into the middle of the nozzle channel. This formed laser sheet had a height of 20 mm and a thickness of only 120 to 200 µm in the vicinity of the nozzle channel. XeF-Excimer laser with an emission wavelength of 351 nm (Compex 150, 2-color-mode, Lambda-Physik) were used as light sources. The lasers were fired with temporal delays between 0.5 and 10 µs and the duration of the pulses were approximately 20 ns. This short exposure time allows the system to freeze and image even very fast processes. The advantage of excimer lasers instead of Nd:YAG lasers which are most often used in PIV setups [6] is the short coherence length of the excimer lasers. So the images of the illuminated tracer particles are not superimposed by speckle patterns. A high resolution dual-frame CCD-camera (12 bit dynamic range, 1280x1024 pixels per frame) equipped with a long-distance microscope (QUESTAR QM100) was mounted perpendicular to the laser sheet plane and captured for each measurement the two separated images of the laser-illuminated tracer particles inside of the nozzle flow. A commercial PIV software (DaVis 6 , LaVision GmbH) was used to calculate the velocity field which resulted of each image pair by using standard cross-correlation PIV algorithms.

The instability of the free liquid film was investigated with two different methods. Back-lit photographs were taken using a short-time flash lamp (NANOLITE), a light diffuser and a CCD-camera with macro objective. In order to have a closer look at the surface waves and especially their depth, a light-sheet-fluorescence technique was used. For this, the laser sheet was focused perpendicular through the liquid film just below the nozzle exit. A CCD-camera with a long-distance microscope was mounted at a detection angle of 36° in respect to the liquid surface. Another CCD-camera with a macro objective was mounted at a detection angle of 59° to detect a larger field of view with less resolution. Figure 2 shows this setup in top view. The quite large detection angle was necessary to avoid blocking or distorting influences from the rim of the liquid film. The water was dyed with a fluorescence dye (Rhodamin 6G) and the objectives were equipped with spectral filters in order to suppress laser light reflection from the roughened film surface. So, only fluorescence light from inside the liquid film excited by the laser sheet was detected, resulting in perpendicular sections through the film. Figure 2 shows an example of such a light-section 3 mm below the nozzle exit (nozzle B) at *Re* = 5500, taken with the long-distance microscope. The blank area represents the fluid. It has to be mentioned that only one of both liquid surfaces was imaged undistorted by this technique (left hand surface in Fig. 2) because the other surface was seen through the roughened liquid film.

In most recent investigations the setup of figure 2 was modified in order to perform PIV measurements of the induced air flow in the vicinity of the liquid film just below the nozzle exit. A dual-frame CCD-camera with a macro objective was used with a detection angle of 5°. In this case not the liquid was dyed but the surrounding air was seeded with a fluorescent aerosol, generated by an atomizer aerosol generator (ATM 210/H, Topas GmbH) using a solution of polyethylene glycol with Rhodamin 6G. The double pulse excimer-laser setup described above was used as the light source for the laser sheet. The velocity fields were calculated with the mentioned PIV software.

Three different nozzle designs were used in this study. They are sketched in Figure 3 and referred as nozzle A, B and C. Nozzle A was made of synthetic quartz glass, nozzles B and C were made of a special UV-transparent acrylic glass (GS 2458, Röhm). Except of the nozzle channel, the nozzle geometry was the same for all nozzle types. The inlet was 12 mm high and 22 mm wide. The length of the contraction zone was 30 mm. The nozzle channel of nozzle A had a length of 19 mm and a height of 0.5 mm. The channels B and C had the same dimensions of 5 mm length and 0.69 mm height. The only difference was a 0.1 mm thick cylindrical wire that was stretched across the channel width (in z-direction) in the middle of the channel height, 3 mm in front of the nozzle exit of nozzle C. In fact nozzle B was nozzle C with removed wire.

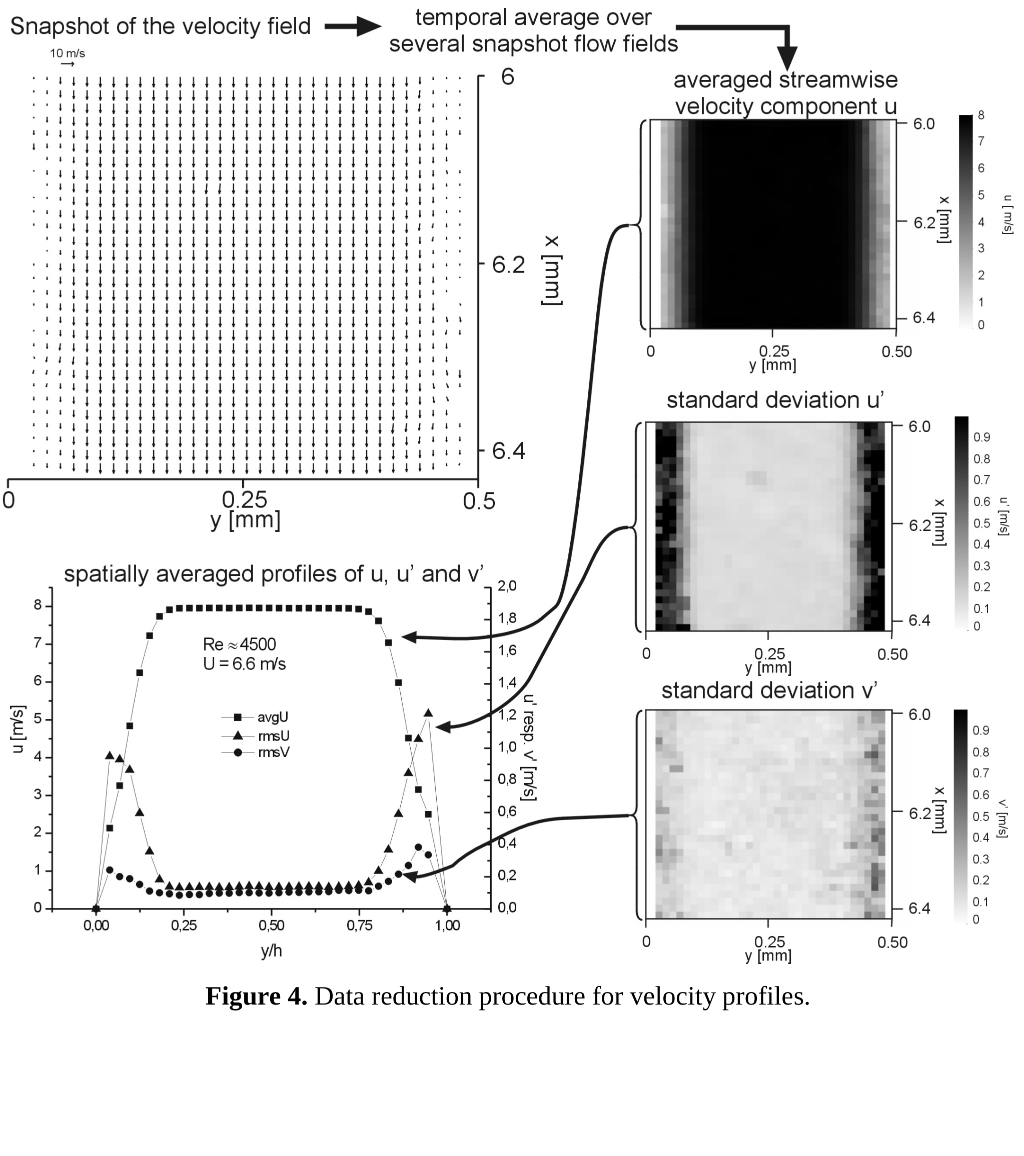

Figure 4. Data reduction procedure for velocity profiles.

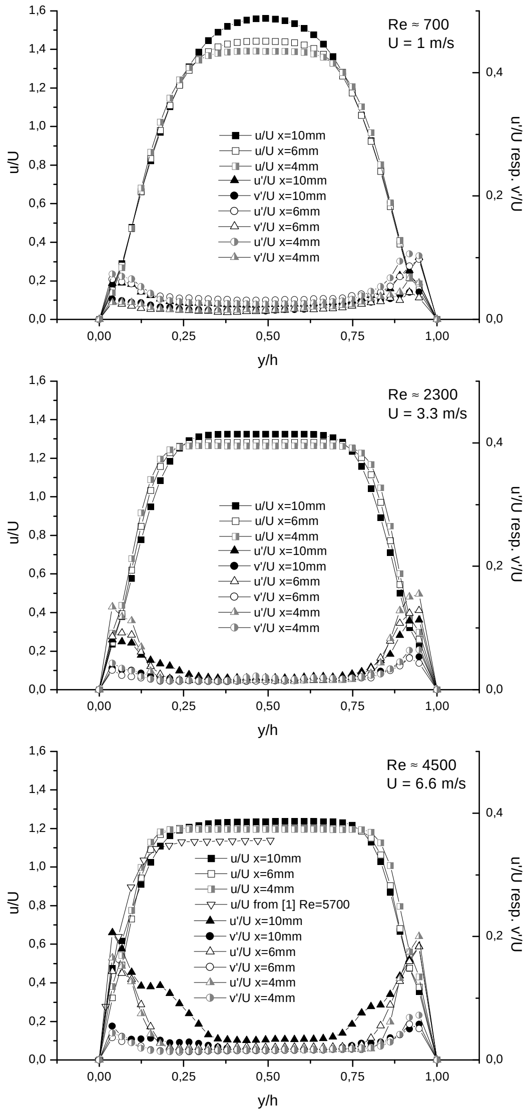

Figure 5. Velocity profiles of nozzle A.

Experimental results

In the case of nozzle A, the dependence of the velocity field on the distance from the end of the contraction zone was examined. 20 snapshots of the velocity field were taken at three different distances (x = 4, 6 and 10 mm, see Figure 3) and at three different flow conditions ($Re \approx 700$, 2300 and 4500, the characteristic length is the channel height h). These 20 snapshot flow fields were averaged for each experimental condition to a temporal average velocity field. These averaged fields were analyzed concerning the main streamwise flow velocity u, its standard deviation u' and the standard deviation v' of the velocity component in y-direction. Velocities could only be measured with a distance greater than 0.02 mm to the walls, so the velocity was set to 0 directly at the walls. For a better understanding, the calculated 2-dimensional fields of $u(x,y)$, $u'(x,y)$ and $v'(x,y)$ were spatially averaged over approximately 0.4 mm along the x-direction. Figure 4 illustrates this data reduction procedure exemplarily for the measurement at x = 6 mm and $Re \approx 4500$. The results are profiles of $u(y)$, $u'(y)$ and $v'(y)$ along the channel height h.

Figure 5 shows the measured velocity profiles at three different x-positions of nozzle A for three different Re numbers. The profiles were normalized by the corresponding average streamwise velocity U. At Re = 700 the typical development of a laminar flow profile could be observed along the channel length in x-direction. The fluctuations u'/U resp. v'/U, which display the current turbulence level, are in the range of the system noise in this case (u'/U resp. $v'/U < 0.05$). In the case of Re = 2300 the profiles show the development of a velocity plateau in the middle of the channel height. The fluctuation in streamwise direction u'/U could only be measured near the walls, whereas v'/U still remained in the range of the detection limit. At higher Re numbers (Re = 4500) the edges of the velocity profiles get steeper and the plateau wider. This observation is supported by the LDV measurements of Heukelbach and Tropea [1] in the channel of a quite similar nozzle. Their velocity profile at Re = 5700 is also included in the graph at the bottom of figure 5. The fluctuations u'/U near the walls are clearly higher at Re = 4500 than at lower Re numbers, whereas the fluctuations spread out towards the middle of the channel with increasing x-distance, namely at x = 10 mm. Again, the fluctuations in spanwise direction v'/U are clearly smaller than in streamwise direction. Only close to the walls v'/U could be measured above the detection

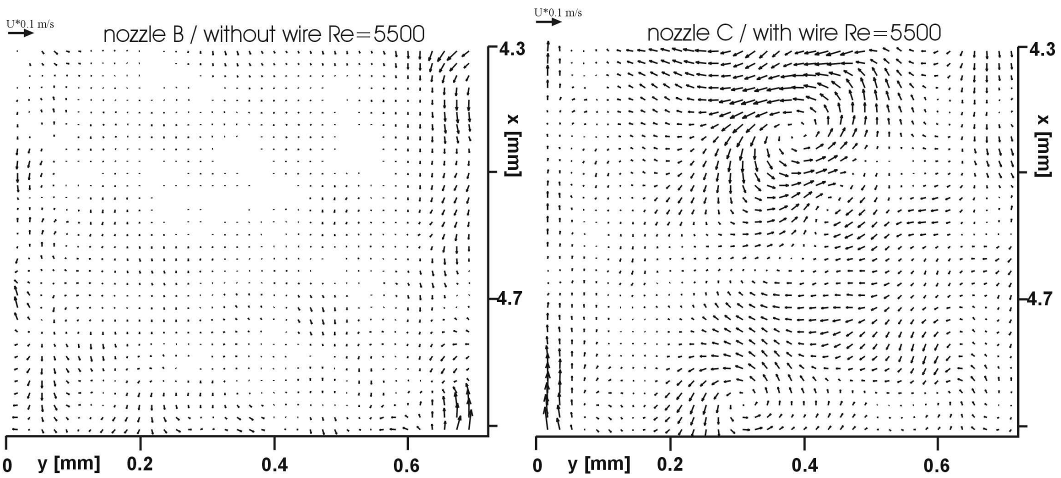

Figure 6. Velocity field of nozzle B (left) and C (right) after Reynolds decomposition.

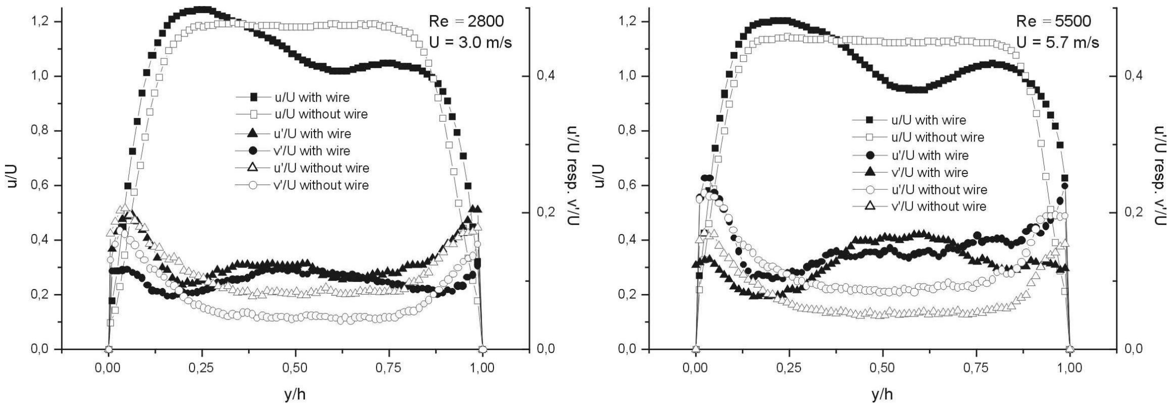

Figure 7. Velocity and fluctuation profiles for nozzle B (without wire) and nozzle C (with wire).

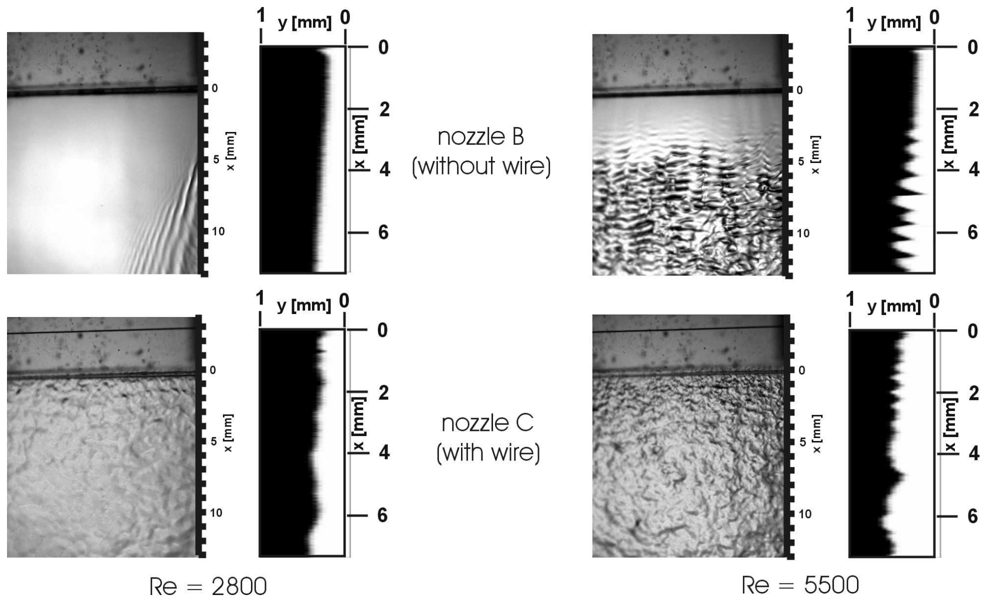

Figure 8. Back-lit photographs of the liquid film and light-sections through the film for nozzle B and C.

limit. The profiles at all flow conditions of figure 5 show a development along the channel length *x*, so the channel flow is not yet completely established at the examined conditions.

The investigations of nozzles B and C show the influence of a micro flow obstacle introduced into the channel flow. The PIV measurements were conducted close to the channel exit (beginning at x = 4.3 mm distance to the contraction zone) at Re ≈ 2800 and 5500. Figure 6 shows the deviation from the corresponding time average velocity field (Reynolds decomposition) of two velocity snapshots without (left) and with (right) inserted wire. The differences of the flow fields, especially the eddy structure in the middle of nozzle C induced by the wire become quite obvious. The influence of the wire can be seen as well from the velocity profiles in figure 7 (calculated as described above). With inserted wire the streamwise velocity *u* gets a break-in near the center of the channel and the fluctuations – even the spanwise component *v'* – are clearly increased in the center region. The profiles of nozzle C are more pronounced at *Re* = 5500 than at *Re* = 2800. The asymmetry in the profiles is most likely due to a not perfectly centered installation of the wire.

Figure 8 shows the effect of the inserted wire on the free liquid film stability. The back-lit photographs for nozzle B at *Re* = 2800 show a smooth liquid surface and at *Re* = 5500 surface waves occur not until 2 mm below the nozzle exit. The light-section shows the growth of these waves. In contrast, with inserted wire (nozzle C) surface waves can be found at the complete liquid film even at the nozzle exit and at low *Re* numbers. The wavelength and amplitudes appear more irregularly which becomes most obvious from the corresponding light-sections in figure 8, whereas amplitudes and frequencies seem to increase with increasing *Re* number and frequencies seem to decrease with increasing distance to the nozzle exit. These observations of the liquid film are in very good accordance with the results of Heukelbach and Tropea [1] who investigated the liquid film stability of similar slit nozzles at similar flow conditions.

Additionally, most recent investigations were conducted on the air flow in the vicinity of the free liquid film which is induced by the liquid flow itself. Figure 9 shows one of the first PIV results for nozzle A at *Re* ≈ 13000

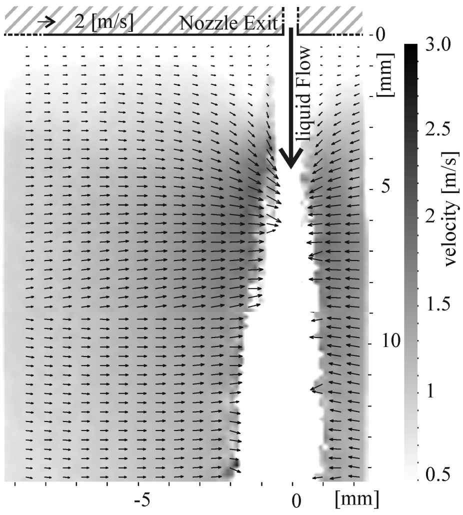

Figure 9. Temporally averaged air flow field at the exit of nozzle A at *Re* ≈ 13000

(of the liquid). Unfortunately, the air flow could only be measured with a minimum distance of approximately 1 mm towards the liquid surface and detaching ligaments blocked the sight further downstream. So, the boundary layer with a flow parallel to the liquid flow is missing in figure 9. Nevertheless, it can be noticed that the flow field of the air is quite inhomogeneous near the nozzle exit.

Conclusions

The experimental results show that it was possible to measure reliable 2 dimensional flow fields inside of nozzle channels with a height of a few hundred micrometers at flow velocities of several meters per second using PIV. The measured velocity profiles for nozzle A show the development of a laminar respectively partly turbulent channel flow which is not yet completely established under the examined conditions. The fluctuations in streamwise direction *u'* could only be measured in the boundary layer at elevated *Re* numbers and spread out towards the center flow only at longer distances from the end of the contraction zone. So, the flow just starts to develop a turbulent profile. These results agree very well with the LDV measurements of Heukelbach and Tropea [1]. Additionally, the PIV measurements show experimentally that the level of the spanwise fluctuations *v'* is clearly smaller than the fluctuations in streamwise direction for this type of nozzle. The investigations of nozzle B and C demonstrate the influence of structural variations of the nozzle on the inner flow field and on the free liquid film. A comparison of the velocity fields after Reynolds decomposition for both nozzles shows the pronounced eddy structure in the center of the flow which is induced by the inserted wire. This elevated turbulence level becomes even more obvious from the corresponding velocity profiles. The profiles of nozzle B are qualitatively similar to those of nozzle A: fluctuations are mainly found in the boundary layer and the component in streamwise direction *u'* is dominant. With inserted wire (nozzle C), there is a high level of fluctuations in the center of the flow and the component *v'* normal to the nozzle walls is of the same magnitude as *u'* in streamwise direction. Regarding the corresponding liquid sheet observations, the influence of the internal flow field on the liquid film becomes obvious. For nozzle B with the low turbulence level the film is smooth at the nozzle exit and only at higher *Re* numbers the growth of surface waves can be observed further downstream. This situation can be explained by linear instability analysis: small disturbances are amplified along the flow mainly driven by aerodynamic forces. For nozzle C with the higher turbulence level the situation is different. The surface is irregularly roughened directly after the nozzle exit, even at low *Re* numbers where aerodynamic effects should be neglected. Obviously, the high level velocity fluctuations are able to disturb the surface effectively. The velocity fluctuations *v'* normal to the walls are assumed to play a dominant roll in these processes. These results are again in good accordance with recent experiments of Heukelbach and Tropea [1].

The first results of PIV experiments on the air flow in the vicinity of the liquid sheet of nozzle A show that this airflow is not simple structured at all, in contrast to the assumption of linear instability analysis. It is expected that these experiments and further analysis of the surface waves (depth and amplitude) will help to clarify discrepancies between experiment and theory and can serve as input or validation of numerical simulation.

References

[1] Heukelbach, K., Tropea, C., “Influence of the inner flowfield of flat fan pressure atomizers on the disintegration of the liquid sheet”, *ILASS-Europe 2001*, Zurich, Switzerland, September 2001.

[2] Lefebvre, A.H., *Atomization and Sprays*, Hemisphere, 1989.

[3] Li, X., “Spatial Instability of Plane Liquid Sheets”, *Chem. Eng. Sci.*, Vol. 48, No. 16, 2973 – 2981, (1993).

[4] Klein, M., Sadiki, A., Janicka, J., “Untersuchung des Einflusses der Düseninnenströmung auf den primären Zerfall eines Flüssigkeitsfilms mittels direkter numerischer Simulation”, *Spray 2001*, Hamburg-Harburg, Germany, November 2001.

[5] Vargaftik, N.B., Vinogradov, Y.K., Yargin, V.S., *Handbook of Physical Properties of Liquids and Gases*, 3rd edition, Begell House inc. publishers, 1996.

[6] Raffel, M., Willert, C., Kompenhans, J., *Particle Image Velocimetry*, Springer, 1998.